Formation of Enamines via Catalytic Dehydrogenation by Pincer-Iridium Complexes

Yansong J. Lu, Xiawei Zhang, Santanu Malakar, Karsten Krogh-Jespersen, Faraj Hasanayn, and Alan S. Goldman*

ACCESS | Metrics & More | Article Recommendations | SI Supporting Information

ABSTRACT: Di-isopropylphosphino-substituted pincer-ligated iridium catalysts are found to be significantly more effective for the dehydrogenation of simple tertiary amines to give enamines than the previously reported di-*t*-butylphosphino-substituted species. It is also found that the di-isopropylphosphino-substituted complexes catalyze dehydrogenation of several β-functionalized tertiary amines to give the corresponding 1,2-difunctionalized olefins. The di-*t*-butylphosphino-substituted species are ineffective for such substrates; presumably, the marked difference is attributable to the lesser crowding of the di-isopropylphosphino-substituted catalysts. Experimentally determined kinetic isotope effects in conjunction with DFT-based analysis support a dehydrogenation mechanism involving initial pre-equilibrium oxidative addition of the amine α-C−H bond followed by rate-determining elimination of the β-C−H bond.
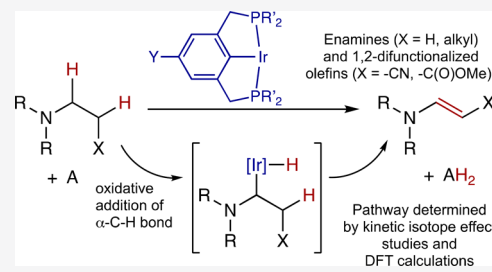
1. INTRODUCTION

The ability to effect selective catalytic conversions of typically unreactive C−H bonds has emerged as one of the major frontiers in organic chemistry in recent years, offering the promise of simple atom-economical methods for the synthesis of valuable functionalized organic compounds.[1] Pincer-ligated iridium complexes have been studied intensively in this context,[2] mostly as highly active and robust catalysts for the dehydrogenation of alkanes, but also for the dehydrogenation of aliphatic C−C linkages in molecules other than alkanes. We have previously reported[3] the synthesis of enamines via dehydrogenation of the corresponding tertiary amines catalyzed by (^{tBu4}PCP)Ir (**1**, ^{R4}PCP = κ^3-C$_6$H$_3$-2,6-(CH$_2$PR$_2$)$_2$),[4] using a sacrificial hydrogen acceptor (Scheme 1). Enamines are highly valuable synthons, used extensively as nucleophiles for the selective formation of C−C bonds by Michael reactions, as Diels−Alder dienophiles, and in a wide range of other reactions.[5]

Subsequent to the early pincer-Ir dehydrogenation work with precursors of (^{tBu4}PCP)Ir,[4,6] it was found that precursors of (^{iPr4}PCP)Ir (**2**) and derivatives are often catalytically more active.[7,8] In this article, we report that (^{iPr4}PCP)IrH$_n$ (n = 2, 4)[7a,8] and the corresponding *p*-methoxy-substituted derivative (MeO-^{iPr4}PCP)IrH$_n$ (**3**)[9] are significantly more effective than (^{tBu4}PCP)IrH$_2$ as catalysts for dehydrogenation of tertiary amines to enamines. We also report that with these sterically much less demanding catalysts, we are able to dehydrogenate crowded 1,2-difunctionalized saturated C−C linkages. This represents a novel approach to the corresponding 1,2-difunctionalized olefins, which are attractive precursors for further functionalization reactions such as cycloadditions, leading to building blocks that cannot be efficiently synthesized via known methods.

We also report herein the results of combined mechanistic experimental and computational (DFT) studies. In conjunction, these results support a mechanism for amine dehydrogenation, which proceeds analogously to that for alkane dehydrogenation but with a lower activation barrier. Specifically, the results are strongly indicative of a pathway operating via addition of an amine α-C−H bond, followed by rate-determining elimination of a hydrogen atom at the amine β-position.
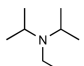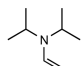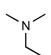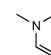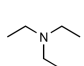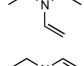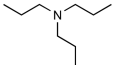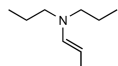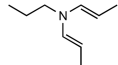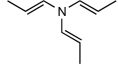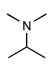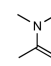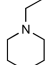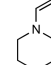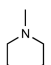
Scheme 1. Reported Synthesis of Enamines via Catalytic Dehydrogenation
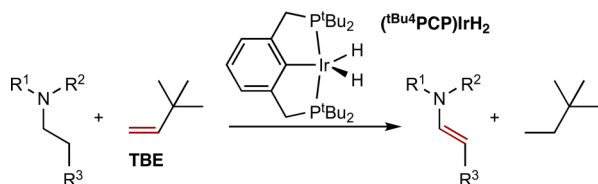
Table 1. Dehydrogenation of Tertiary Amines Catalyzed by (MeO-^{iPr4}PCP)IrH$_n$ (with Previously Reported[3] Results Obtained with (^{tBu4}PCP)IrH$_2$ Shown for Comparison)[a]

Entry	Substrate (0.1 M)	Product	(MeO-^{iPr4}PCP)IrH$_2$ Conditions (120 °C)	Yield (%)	(^{tBu4}PCP)IrH$_2$[3] Conditions (90 °C)	Yield (%)
1	(structure)	(structure)	48 h, 2 equiv NBE, 1% cat.	90	5 h, 2 equiv TBE, 10% cat.	98
					24 h, 2 equiv TBE, 2% cat.	65
2	(structure)	(structure)	32 h, 2 equiv NBE, 2% cat.	95	24 h, 2 equiv TBE, 10 % cat.	65
3	(structure)	(structure)	32 h, 4 equiv NBE, 2% cat.	53	24 h, 3 equiv TBE, 10% cat.	25
		(structure)		40		75
4	(structure)	(structure)	32 h, 4 equiv NBE, 2% cat.	40	24 h, 2 equiv TBE, 10 % cat.	43
		(structure)		38		11
		(structure)		6		-
5	(structure)	(structure)	32 h, 2 equiv NBE, 2% cat.	39	24 h, 2 equiv TBE, 10 % cat.	10
6	(structure)	(structure)	48 h, 2 equiv NBE, 2% cat.	90	24 h, 3 equiv TBE, 10% cat.	67
					24 h, 2 equiv NBE, 10% cat.	92
7	(structure)		48 h, 2 equiv NBE, 2% cat.	N.R.	24 h, 2 equiv TBE, 10 % cat., 110 °C	N.R.

[a]All reactions were conducted with 0.1 M amine substrate in *p*-xylene-d_{10} solvent and were monitored by ^{31}P NMR and ^{1}H NMR spectroscopies over the course of the reaction. Yields were determined by ^{1}H NMR spectroscopy.

2. RESULTS AND DISCUSSION

2.1. Dehydrogenation of Tertiary Amines. In our previous report of the transfer dehydrogenation of tertiary amines catalyzed by (^{tBu4}PCP)IrH$_n$,[3] we found that a relatively high catalyst loading was generally required to obtain good yields. With (^{iPr4}PCP)IrH$_n$ and the same substrates investigated previously, using NBE as a hydrogen acceptor, satisfactory yields were generally achieved with a catalyst loading of only 2%, although higher temperatures and somewhat longer reaction times were generally required (Table 1). Note that with these same higher reaction temperatures and longer times, with (^{tBu4}PCP)IrH$_n$ (as opposed to (^{iPr4}PCP)IrH$_n$), the yields of the reactions were actually lowered, not increased. The need for higher temperature with (^{iPr4}PCP)IrH$_n$ is likely a consequence of stronger binding of olefin (either H-acceptor or enamine) to the sterically less demanding catalyst. Very high yields obtained with (^{iPr4}PCP)IrH$_n$, much higher than with (^{tBu4}PCP)IrH$_n$, have also been reported for alkane transfer dehydrogenation using the strongly binding hydrogen acceptors ethylene and propylene; in this case too, the optimal temperatures (>200

°C) are significantly higher than those found for (^{tBu4}PCP)-IrH$_n$.[7c]

In general, the same reactivity patterns were observed with (MeO-^{iPr4}PCP)Ir as with (^{tBu4}PCP)Ir. This includes complete selectivity for dehydrogenation of an *N*-ethyl group versus an *N*-*i*-propyl group (entry 1) and the failure to dehydrogenate the piperidine ring in either *N*-methylpiperidine or *N*-ethylpiperidine. The greater effectiveness of (MeO-^{iPr4}PCP)Ir as compared with (^{tBu4}PCP)Ir, however, was much more marked for the dehydrogenation of *n*-propyl groups (entry 4) and the *i*-propyl group (entry 5). This is likely attributable to lesser crowding at the metal center of (MeO-^{iPr4}PCP)Ir, relative to (^{tBu4}PCP)Ir, being particularly favorable for dehydrogenation of C–C linkages more crowded than the ethyl group.

As observed with (^{tBu4}PCP)Ir-catalyzed reactions, all of the enamine products degraded, usually within several hours, after being isolated from the catalyst (via vacuum transfer of enamine and solvent); this behavior is consistent with the known instability of simple enamines.[5a,10] Thus, it is remarkable that the enamines are stable at the high temperature (120 °C) at which they are formed. In view of

that stability at elevated temperatures, however, it is not surprising that the enamines are indefinitely stable, while still in the presence of the Ir complex, at room temperature. As previously[3] proposed, it seems probable that the Ir complex inhibits a chain reaction leading to loss of the enamine, perhaps by scavenging chain initiators.

2.2. Dehydrogenation To Afford 1,2-Difunctional Olefins.

1,2-Difunctional olefins are of great interest as versatile intermediates in organic synthesis for various cycloadditions.[11] Electron-rich 1,2-difunctional olefins in particular can undergo useful [2 + 1] cycloadditions (cyclopropanation, Simmons–Smith type reaction)[12] and [2 + 2],[13] [3 + 2],[14] and [4 + 2][15] cycloadditions, to afford various compounds that serve as novel building blocks for organic synthesis.

In this context and that of tertiary amine dehydrogenation, we considered the dehydrogenation of β-functionalized tertiary amines. We first attempted the catalytic dehydrogenation of the relatively sterically hindered diamine substrate, N,N,N',N'-tetramethyl-ethane-1,2-diamine (tetramethylethylenediamine; TMEDA) (eq 1). Various conditions were screened, including the use of NBE, TBE, and camphene as hydrogen acceptors; significant yields of the desired product were achieved only with NBE.[16]

$$ \text{(1)} $$
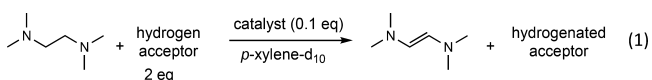
Catalysts **1–5** (Scheme 2) were screened for the reaction outlined in eq 1; among these catalysts, **2** and **3** proved to be similarly effective. Catalyst **1** gave no observable product, presumably highlighting the importance of steric factors for dehydrogenation of this sterically hindered substrate (TMEDA). Catalyst **4** gave some product but less than **2** or **3**. Catalyst **5** apparently polymerized the hydrogen acceptor (NBE),[17] and the desired dehydrogenation products were not detected.

Other 1,2-difunctionalized ethane derivatives were investigated. Vinyl acrylates have been found to form stable, catalytically inactive, adducts with (^{tBu4}PCP)Ir.[18] We were therefore pleasantly surprised that some, albeit limited, catalytic dehydrogenation of methyl 3-(dimethylamino)-propanoate (entry 4) was achieved, likely due to steric hindrance preventing the formation of such inactive adducts. Relatedly, nitriles appear to coordinate fairly strongly to (^{R}PCP)Ir fragments, yet a very good yield (84%) was obtained with the substrate 3-(dimethylamino)propanenitrile (entry 5).

Our previous attempts to dehydrogenate ethers have for the most part been unsuccessful apparently due to the formation of vinyl ether adducts. Some success has been achieved with ether dehydrogenation.[19] Most notably in the context of this work, Brookhart and co-workers found that (^{iPr4}PCP)Ir could effect dehydrogenation of acyclic ethers,[20] and Huang and co-workers reported[21] dehydrogenation of cyclic amines and ethers with the related (^{iPr4}PSCOP)Ir species. Inspired by the

success noted above with 1,2-difunctionalized substrates such as TMEDA, we attempted dehydrogenation of a bulky bis(trimethylsilyl)diether substrate (entry 6) and were pleased to obtain excellent yields.

Entries 1, 4, 5, and 6 in Table 2 represent new chemical transformations. Only a single isomer (E) was obtained from each of the four reactions, as indicated in Table 2.

N,N'-Dimethyl-N,N'-dibenzyl-ethylene-1,2-diamine did not undergo any reaction (entry 2), which is likely attributable to steric hindrance by the benzyl substituents as compared with the methyl groups. 1,4-Dimethylpiperazine did not undergo dehydrogenation (entry 3) in accordance with the failure, reported above, to dehydrogenate N-methylpiperidine and N-ethylpiperidine at the ring position.

2.3. Mechanistic Studies.

The apparently high reactivity of the acyclic amine substrates, indicated by the good product yields, was confirmed in a competition experiment between N,N-di(isopropyl)ethylamine (60 mM) and cyclooctane (COA; 600 mM) (Scheme 3).[3,22] The latter substrate is frequently used in alkane dehydrogenation studies because of its anomalously low enthalpy of dehydrogenation.[2,4,6]

The reaction was conducted as a stoichiometric competition reaction of (^{tBu4}PCP)Ir(H)(Ph) (which is known to act as an effective precursor of the fragment (^{tBu4}PCP)Ir even at or below room temperature[23]), in the absence of the hydrogen acceptor, allowing characterization by ^{1}H NMR spectroscopy at very low conversions of COA and di(isopropyl)ethylamine. This procedure favored the observation of cyclooctene and N,N-di(isopropyl)vinylamine in a kinetically determined ratio rather than a thermodynamic distribution. Indeed, the ratio of cyclooctene to N,N-di(isopropyl)vinylamine remained roughly constant at 1:2.0, even from the earliest reaction times. Dehydrogenation of the $^iPr_2$NEt ethyl group is thus found (after accounting for the 10:1 excess of COA) to be 20 times more rapid than dehydrogenation of COA on a per mole basis; on a per C–C bond basis, the ratio is therefore 160.[3]

Competition experiments between N,N-di(alkyl)ethylamines reveal that the rate of dehydrogenation of the N-ethyl group is dependent upon the ancillary N-alkyl group as follows: i-propyl > ethyl > methyl in the ratio of approximately 140:7:1.[3] The trend is opposite to what would be expected based on consideration of steric factors. It is not obvious how this trend would be reconciled with the generally accepted reaction pathway for alkanes, which proceeds via oxidative addition followed by β-hydrogen elimination.[2] More generally, the origin of the much greater reactivity of amines compared with alkanes is not obvious in the context of such a mechanism. We therefore considered that alternative pathways might be operative, proceeding, for example, via radicals or via electron transfer.

To address this fundamental mechanistic question, we first conducted a series of kinetic isotope effect (KIE) experiments. N,N-di(isopropyl)ethylamine isotopologues $^iPr_2N(CD_2CD_3)$, $^iPr_2N(CD_2CH_3)$, and $^iPr_2N(CH_2CD_3)$ were synthesized. In a competitive catalytic reaction (90 °C), (^{tBu4}PCP)IrH$_n$ (10.2
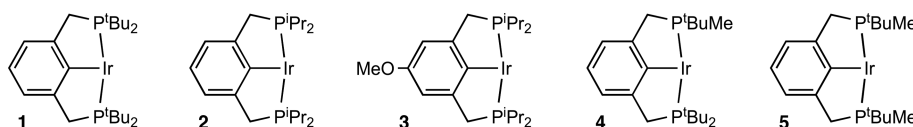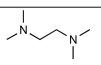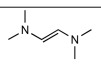
Scheme 2. Pincer-Iridium Catalysts Screened
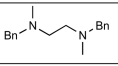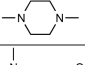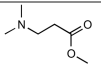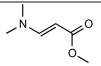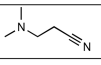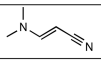
Table 2. Dehydrogenation Reactions Catalyzed by (^{iPr4}PCP)Ir (2) with NBE as Hydrogen Acceptor[a]

Entry	Substrate	Product	Conditions	Yield (%)
1			A	64%
			B	98%
2			A	N.R.
3			A	N.R.
4			A (110 °C/55 h)	27
5			A	84
6			A (110 °C/40 h)	96 E/Z = 6.5/1
			(110 °C/70 h)	100 E/Z = 10/1

[a]All reactions were run in p-xylene-d_{10}, and NBE was used as a hydrogen acceptor. All yields were determined by ^{1}H NMR spectroscopy. **A**: 0.05 mmol substrate (0.1 M), 2.3 equiv (0.115 mmol) NBE, 15 mol % (4.0 mg) **2**, 143 °C, 45 h, unless noted otherwise. **B**: 0.05 mmol substrate (0.1 M), 2.0 equiv (0.10 mmol) NBE, 25 mol % (6.6 mg) **2**, 143 °C, 24 h.

Scheme 3. Competition Experiment To Determine Relative Reactivity of COA versus ^{i}Pr$_2$NEt
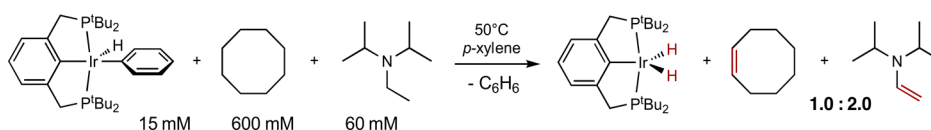
Scheme 4. Pathway for Amine Dehydrogenation by 1 Consistent with Observed Isotope Effects
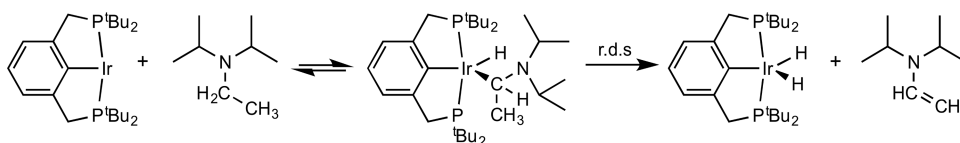
mM), TBE (250 mM), ^{i}Pr$_2$N(C$_2$H$_5$) (30.7 mM), and ^{i}Pr$_2$N-(C$_2$D$_5$) (61.4 mM) were allowed to react; k_{C2H5}/k_{C2D5} was found to be 7.0.[3] A stoichiometric competition reaction with (^{tBu4}PCP)Ir(H)(Ph), conducted in analogy with the above described experiment with COA (Scheme 3), was conducted with ^{i}Pr$_2$N(C$_2$H$_5$) (146 mM) and ^{i}Pr$_2$N(CH$_2$CD$_3$) (291 mM) and was found to give a KIE of k_{C2H5}/k_{CH2CD3} = 3.7. In another such stoichiometric competition reaction, the reaction of (^{tBu4}PCP)Ir(H)(Ph) with ^{i}Pr$_2$N(C$_2$H$_5$) (146 mM) and ^{i}Pr$_2$N-(CD$_2$CH$_3$) (291 mM), the value of k_{C2H5}/k_{CD2CH3} was found to be 2.0. Thus, k_{C2H5}/k_{C2D5} (7.0) is approximately equal to the product of the KIE values k_{C2H5}/k_{CH2CD3} (3.7) and k_{C2H5}/k_{CD2CH3} (2.0).

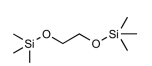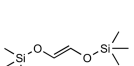The results of these isotope effect experiments clearly imply that cleavage of both α- and β-C−H bonds occurs during or preceding the rate-determining step. Thus, they argue against a mechanism proceeding via rate-determining electron transfer or abstraction of an H atom from the amine.

The value of 2.0 for k_{C2H5}/k_{CD2CH3} is consistent with an equilibrium isotope effect (preceding a rate-determining step) for a reaction in which H is transferred from carbon to a metal atom, while the value of 3.7 for k_{C2H5}/k_{CH2CD3} indicates a rate-limiting kinetic isotope effect.[24] These isotope effects are thus consistent with a pathway featuring reversible oxidative addition of the α-C−H bond followed by rate-determining β-H-elimination (Scheme 4). It is still not obvious, however, why such a mechanism would favor amines over alkanes. In

this context, we conducted a computational study to elucidate the detailed energetics of this putative reaction mechanism.

2.4. Computational Studies. A series of electronic structure calculations based on density functional theory (DFT; M06 level, see Computational Methods) were conducted for dehydrogenation pathways proceeding through oxidative addition of an aminoethyl C−H bond of ^{i}Pr$_2$NEt or Me$_2$NEt to (^{tBu4}PCP)Ir, followed by β-H elimination to give the corresponding vinyl amines. We also calculated, for comparison, the energy profiles of pathways for dehydrogenation of COA and n-butane and for the alkanes that are isostructural with ^{i}Pr$_2$NEt and Me$_2$NEt, namely, 3-ethyl-2,4-dimethylpentane and isopentane, respectively (corresponding products shown in Scheme 5). For all of these substrates except COA, two distinct dehydrogenation pathways of this type are possible, and both were investigated computationally (Scheme 6): pathway **a**, oxidative addition of a primary C−H bond followed by β-H-elimination of the adjacent secondary

Scheme 5. Products of Dehydrogenation of Various Substrates for Which Dehydrogenation Pathways Were Calculated
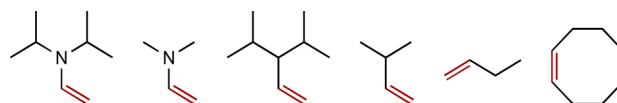
Scheme 6. Putative Pathways for Dehydrogenation of Amines and Alkanes Examined by DFT Calculations
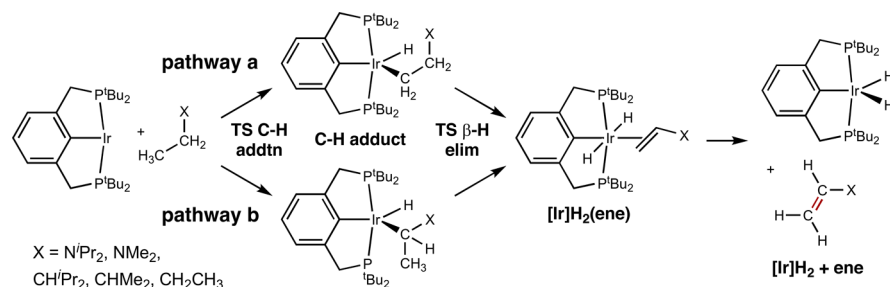
C–H bond, and pathway **b**, oxidative addition of the secondary C–H bond followed by β-H-elimination of the adjacent primary C–H bond.

For all substrates and for either pathway, the energy of the TS for the second step, β-H elimination, is higher than that for the first C–H activation step. Thus β-H-elimination is calculated to be the rate-determining step for the formation of trans-(^{tBu4}PCP)IrH$_2$(olefin) ([**Ir**]**H**$_2$(**ene**)). The Gibbs free energies (relative to (^{tBu4}PCP)Ir plus free substrate) of the TS for the C–H addition, the C–H addition intermediate, the TS for β-H-elimination, the intermediate trans-(^{tBu4}PCP)-IrH$_2$(olefin), and the free olefin product plus (^{tBu4}PCP)IrH$_2$ are given in Table 3.

Table 3. Calculated Gibbs Free Energies (kcal/mol; 50 °C; 1.0 M Substrate) of Key Intermediates and TSs for Dehydrogenation of Various Substrates via Pathways a and b Outlined in Scheme 6

substrate	pathway	TS CH-addtn	C–H adduct	TS β-H-elim	[Ir]H$_2$(ene)	[Ir]H$_2$ + ene
^{i}Pr$_2$NEt	a	20.1	14.2	31.4	20.0	7.1
^{i}Pr$_2$NEt	b	29.9	29.1	32.6	20.0	7.1
Me$_2$NEt	a	19.5	13.2	30.8	20.9	6.0
Me$_2$NEt	b	25.0	23.9	32.0	20.9	6.0
N-Me-piperidine	a	23.8	18.3	36.7	23.7	5.6
N-Me-piperidine	b	28.8	22.7	41.5	23.7	5.6
n-butane	a	22.0	16.1	35.2	22.9	12.3
n-butane	b	29.3	20.9	36.8	22.9	12.3
^{i}Pr$_2$CHEt	a	20.7	17.2	36.3	22.5	11.6
^{i}Pr$_2$CHEt	b	30.3	30.0	32.9	22.5	11.6
Me$_2$CHEt	a	22.8	14.6	34.5	22.3	12.4
Me$_2$CHEt	b	27.5	27.8	36.7	22.3	12.4
COA		27.2	23.4	34.9	28.0	3.7

The calculated free energies shown in Table 3 can be considered in the context of the experimental observations described above. Relative rates for all substrates are determined by the free energy of the TS for β-H-elimination (**TS β-H-elim**); these TS energies are the lowest for the acyclic amines, consistent with the qualitative observation that these amines are more reactive than alkanes. For N-Me-piperidine, **TS β-H-elim** is calculated to be equal or higher in free energy than for the alkanes studied, consistent with its failure to undergo dehydrogenation. More quantitatively, as described above, in the competition experiment between ^{i}Pr$_2$NEt and COA, a relative rate factor of 160 per C–C bond favoring the amine was determined, which corresponds to $\Delta\Delta G^{\ddagger}_{50\,°C}$ = 3.3 kcal/mol. The calculated values of $\Delta\Delta G^{\ddagger}_{50°C}$, 3.5 and 2.2 kcal/mol

for pathways **a** and **b**, respectively, are both in good agreement with this value.

KIEs were calculated for dehydrogenation of the ^{i}Pr$_2$NEt isotopologues that were experimentally investigated. For pathway **a**, at 50 °C, the KIE was calculated to be 2.5 for the terminal position of the aminoethyl group of ^{i}Pr$_2$NEt ($k_{C2H5/CH2CD3}$) and 5.2 for the methylene group ($k_{C2H5/CD2CH3}$); for full isotopic substitution of the ethyl group, $k_{C2H5/C2D5}$ = 13.1 at 50 °C and 9.9 at 90 °C. For pathway **b**, the calculated values are $k_{C2H5/CH2CD3}$ = 3.5, $k_{C2H5/CD2CH3}$ = 2.9, and $k_{C2H5/C2D5}$ = 10.1 (50 °C) and 7.8 (90 °C). The experimental KIEs, discussed above, are $k_{C2H5/CH2CD3}$ = 3.7, $k_{C2H5/CD2CH3}$ = 2.0 (50 °C), and $k_{C2H5/C2D5}$ = 7.0 (90 °C). The experimental values are clearly inconsistent with the values calculated for pathway **a**. Conversely, they are in good agreement with the calculations for pathway **b**; we believe that this agreement offers very strong support for this pathway.

The difference in barrier heights computed for pathways **a** and **b** is, however, small in all cases (1–3 kcal/mol; Table 3), testing the reliability of the computational methods. Indeed, for ^{i}Pr$_2$NEt, pathway **a** is calculated to have a Gibbs free-energy barrier that is 1.3 kcal/mol lower than pathway **b** (Table 3). We consider the magnitude of this discrepancy to be well within the overall limits of uncertainty for the applied computational methodology.[25,26] The rate-determining TS (β-H elimination) obtained for ^{i}Pr$_2$NEt dehydrogenation along pathway **b** is more sterically crowded than the corresponding TS along pathway **a**, and it seems plausible that the incomplete treatment of dispersive interactions offered by the M06 functional contributes to the discrepancy. Similarly, the slightly higher calculated barriers for dehydrogenation of ^{i}Pr$_2$NEt versus Me$_2$NEt ($\Delta\Delta G^{\ddagger}_{50\,°C}$ = approximately 0.6 kcal/mol for either pathway **a** or **b**) may be at least in part due to a very approximate treatment of dispersive interactions.

The calculations offer a straightforward explanation for the selectivity for dehydrogenation of amines compared with alkanes. The energies of the C–H addition products and their barriers to β-H-elimination vary greatly between substrates and pathways. In contrast, the energies of the transition states **TS β-H-elim** (particularly for pathway **b**) correlate fairly well with the energies of the intermediates to which they connect, the β-H-elimination products, [**Ir**]**H**$_2$(**ene**). In particular, the intermediates resulting from acyclic amine dehydrogenation are the lowest in free energy of those in Table 3, as are the corresponding transition states **TS β-H-elim**. Consistent with this correlation of free energies, the geometries of the transition states **TS β-H-elim** are notably similar to those of the intermediates [**Ir**]**H**$_2$(**ene**) as shown in Figure 1 for dehydrogenation of ^{i}Pr$_2$NEt. The product-like nature of **TS β-H-elim** also helps to rationalize why the free energy of this TS is very similar for pathways **a** and **b** despite the fact that the
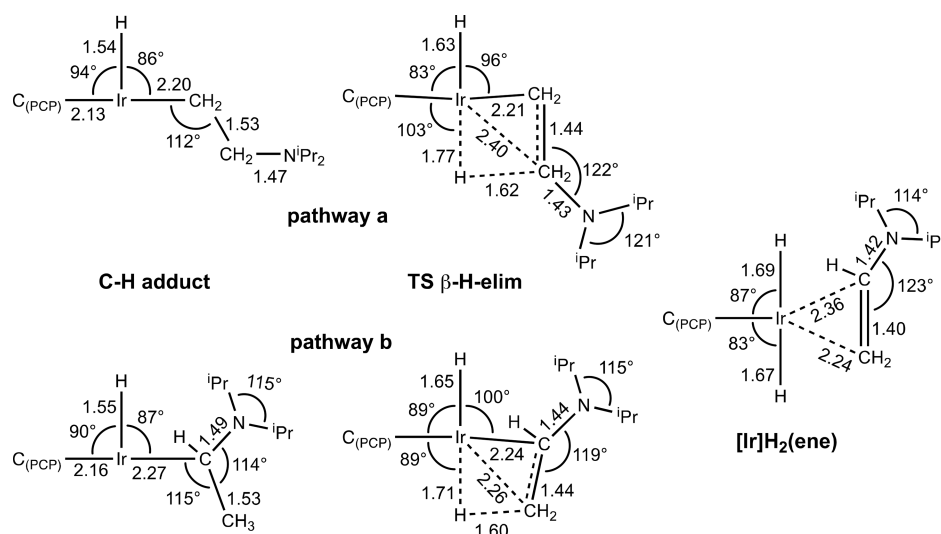
Figure 1. Selected bond distances (in Å) and angles for the products of C−H bond addition (**C−H adduct**), the TSs for β-H elimination (**TS β-H-elim**), and the resulting intermediate ([**Ir**]**H$_2$(ene)**) for the reaction of (^{tBu4}PCP)Ir with ^{i}Pr$_2$NEt via **pathway a** and **pathway b**.

different TSs are derived from C−H addition products, which have very different free energies in the two pathways.

If the variations in the energies of **TS β-H-elim** can be rationalized in terms of the energies of the intermediates, [**Ir**]**H$_2$(ene)**, then the question arises as to what may explain the variations in energies of these intermediates. A comparison between the amines and the isostructural alkanes is probably most informative in this context. We note that the difference between the relative energies of the amine dehydrogenation intermediates and the isostructural alkane dehydrogenation intermediates, [**Ir**]**H$_2$(ene)**, is approximately 2 kcal/mol (Table 3). This compares with a difference of approximately 5 kcal/mol for the relative energies of the free enamine and alkene products, attributable to conjugation between the amino group and the C−C π-system. We presume that the lower energy of the [**Ir**]**H$_2$(ene)** amine dehydrogenation products simply reflects the lower energy of the free dehydrogenated species (with the difference mitigated by stronger binding of the enamine); this same effect is therefore ultimately responsible for the faster kinetics of dehydrogenation of amines compared with alkane. For the cyclic species studied, COA and N-methylpiperidine, in contrast, the corresponding free olefins are low in energy. However, consistent with the relatively low reactivity of these substrates, their corresponding Ir-olefin adducts are higher in free energy than the adducts of the linear olefins, presumably for steric reasons.

3. CONCLUSIONS

Precursors of (^{iPr4}PCP)Ir and (MeO-^{iPr4}PCP)Ir are efficient catalysts for dehydrogenation of simple tertiary amines to give enamines, significantly more effective than precursors of the previously reported, more sterically hindered, (^{tBu4}PCP)Ir fragment. They are also found to catalyze (unlike (^{tBu4}PCP)Ir) the dehydrogenation of β-functionalized tertiary amines to give the corresponding 1,2-difunctionalized olefins, which are of interest for further chemical manipulations such as cyclo-addition reactions.[11−15] Combined mechanistic and computational studies indicate that the amine dehydrogenations proceed via C−H oxidative addition at the N-bound carbon, followed by rate-limiting β-H elimination.

4. EXPERIMENTAL SECTION

4.1. General Information. All reactions, recrystallizations, and routine manipulations were conducted under an inert atmosphere using an argon-filled glove box or by using standard Schlenk techniques under an argon atmosphere. J. Young NMR tubes were used for catalytic dehydrogenation reactions. Reagent grade solvents were used and dried according to established methods and then degassed with argon. All NMR solvents were dried, vacuum-transferred, and stored in an argon-filled glove box.

^{1}H, ^{31}P{^{1}H}, and ^{13}C{^{1}H} NMR spectra were obtained on Varian 300-, 400-, or 500-MHz spectrometers. ^{1}H and ^{13}C NMR chemical shifts are reported in ppm downfield from tetramethylsilane and were referenced to residual protiated (^{1}H) or deuterated solvent (^{13}C). Catalysts **1-H$_n$**,[4] **2-H$_n$**,[7a] **3-H$_n$**,[9] **4-H$_n$**,[7b] and **5-H$_n$**,[7b] and (^{tBu4}PCP)-Ir(H)Ph[23] were prepared as described in the literature. Simple amines were purchased from Sigma-Aldrich. N,N-diisopropylpropylamine and isotopically labeled N,N-diisopropylethylamines i-Pr$_2$N(C$_2$D$_5$), i-Pr$_2$N(CD$_2$CH$_3$), and i-Pr$_2$N(CH$_2$CD$_3$) were synthesized according to a literature procedure.[27] All amines were purified by treating with Na/K alloy, followed by vacuum distillation. All substrates were stored over molecular sieves before use.

4.2. General Procedure for Catalytic Dehydrogenation. All substrates, hydrogen acceptors, catalysts, and solvents were loaded into a J. Young NMR tube in a glovebox under an argon atmosphere. A ^{1}H NMR spectrum was acquired at time zero (t_0), and the NMR tube was heated in an oil bath. The reaction progress was monitored by ^{1}H NMR spectroscopy. Yields were calculated based on relevant peak areas in the ^{1}H NMR spectrum.

For the dehydrogenation of simple tertiary amines, the solvent was removed followed by bulb-to-bulb distillation of the higher-MW products to give a colorless oil that included any unreacted amine and multiply dehydrogenated product as well as monoene. The mixture was subjected to mass spectroscopic as well as NMR analysis, but no attempts were made to isolate the monoene product.[3]

N,N-Di(isopropyl)vinylamine: ^{1}H NMR (300 MHz, p-xylene-d_{10}, δ): 6.10 (dd, 15.6 Hz, 9.2 Hz, 1H), 3.83 (d, 9.2 Hz, 1H), 3.82 (d, 15.6 Hz, 1 H), 3.41 (m, 6.5 Hz, 2H), 1.03 (d, 6.5 Hz, 12H). MS (EI) m/z: 127(parent), 112, 99, 70, 56.[3]

N,N-Dimethylvinylamine: ^{1}H NMR (300 MHz, p-xylene-d_{10}, δ): 6.01 (dd, J_{HH} = 15.2 Hz, 8.4 Hz, 1 H), 3.84 (d, J_{HH} = 8.4 Hz, 1H), 3.74 (d, J_{HH} = 15.2 Hz, 1H), 2.39 (s, 6H). MS (EI) m/z: 71(parent), 58, 56, 44.[3]

N,N-Diethylvinylamine: ^{1}H NMR (300 MHz, p-xylene-d_{10}, δ): 6.03 (dd, J_{HH} = 15.2 Hz, 9.2 Hz, 1H), 3.78(d, J_{HH} = 9.2 Hz, 1H), 3.75(d,

J_{HH} = 15.2 Hz, 1H), 2.81(q, J_{HH} = 7.0 Hz, 4H), 1.05(t, J_{HH} = 7.0 Hz, 6H). MS (EI) m/z: 99(parent), 84, 73, 71, 56.[3]

N,N-Divinylethylamine: ^{1}H NMR (300 MHz, *p*-xylene-d_{10}, δ): 6.00 (dd, J_{HH} = 15.6 Hz, 9.0 Hz, 2 H), 3.93 (d, J_{HH} = 15.6 Hz, 2 H), 3.86 (d, J_{HH} = 9.0 Hz, 2H), 3.14 (q, J_{HH} = 7.0 Hz, 2H), 1.02 (t, J_{HH} = 7.0 Hz, 3 H). MS (EI) m/z: 97(parent), 83, 70, 56.[3]

N,N-Dipropyl-(*E*)-1-propenylamine: ^{1}H NMR (300 MHz, *p*-xylene-d_{10}, δ): 5.89 (dd, J_{HH} = 13.5 Hz, 1.5 Hz, 1H), 4.18 (qd, J_{HH} = 6.3 Hz, 13.5 Hz, 1 H), 2.75 (t, J_{HH} = 7.2 Hz, 4H), 1.85 (dd, J_{HH} = 6.3 Hz, 1.5 Hz, 3H), 1.48 (tq, J_{HH} = 7.2 Hz, 7.2 Hz, 4H), 0.98 (t, J_{HH} = 7.2 Hz, 6H).[3]

N,N-Di-(*E*)-1-propenylpropylamine: ^{1}H NMR (300 MHz, *p*-xylene-d_{10}, δ): 5.91 (d, J_{HH} = 13.6 Hz, 2 H), 5.38 (m, J_{HH} = 13.6 Hz, 6.4 Hz, 2 H), 3.04 (t, J_{HH} = 7.6 Hz, 2 H), 1.75 (d, J_{HH} = 6.4 Hz, 6 H), 1.31 (m, 2H), 1.01 (t, J_{HH} = 6.8 Hz, 3 H). MS(EI) m/z: 139(parent), 124, 110, 98, 70.[3]

N-Vinylpiperidine: ^{1}H NMR (300 MHz, *p*-xylene-d_{10}, δ): 5.99 (dd, J_{HH} = 15.3 Hz, 8.7 Hz, 2H), 3.90 (d, J_{HH} = 15.3 Hz, 1H), 2.88(d, J_{HH} = 8.7 Hz, 1H), 2.68 (t, J_{HH} = 5.3 Hz, 4H), 1.60 (m, 6H).[3]

(*E*)-*N,N,N′,N′*-Tetramethylethene-1,2-diamine: ^{1}H NMR (400 MHz, *p*-xylene-d_{10}, δ): 5.44 (s, 2H), 2.5 (s, 12H).

(*E*)-3-(Dimethylamino)acrylonitrile: ^{1}H NMR (400 MHz, *p*-xylene-d_{10}, δ): 3.49 (d, J = 13.6 Hz, 1H), 6.34 (d, J = 13.6 Hz, 1H), 2.60 (s, 6H).

Methyl (*E*)-3-(Dimethylamino)acrylate: ^{1}H NMR (500 MHz, *p*-xylene-d_{10}, δ): 7.52 (d, J = 13.0 Hz, 1H), 4.80 (d, J = 13.0 Hz, 1H), 3.88 (s, 3H), 3.02 (s, 6H).

(*E*)-2,2,7,7-Tetramethyl-3,6-dioxa-2,7-disilaoct-4-ene: ^{1}H NMR (300 MHz, *p*-xylene-d_{10}, δ): 5.65 (s, 2H), 0.35 (s, 18H).

5. COMPUTATIONAL METHODS

All calculations employed density functional theory (DFT)[28] as implemented in the GAUSSIAN 16 series of computer programs.[29] We applied the M06 functional in the majority of calculations,[30] along with the SDD effective core potential and associated valence basis set for the Ir atom;[31] all other atoms (P, N, C, and H) were assigned all-electron 6-31G(d,p) basis sets.[32] Interactions with the bulk solvent were simulated using the SMD dielectric continuum solvation model[33] and *p*-xylene as the model solvent. Normal mode analysis was performed for stationary points, and thermal energy corrections were evaluated using standard statistical mechanical expressions and unscaled vibrational frequencies.[34] Computed Gibbs free energies were adjusted to a temperature of 50 °C for comparison with experimental data.

■ ASSOCIATED CONTENT

ⓢ Supporting Information

The Supporting Information is available free of charge at https://pubs.acs.org/doi/10.1021/acs.joc.9b02846.

> Computational details, tables of calculated energetic quantities for full pathways, kinetic isotope effect calculations, Cartesian coordinates of DFT optimizations, NMR spectra of unreported amines and reaction mixtures, optimized structures (as .mol2 formatted files) for all pathways considered (PDF)
>
> MACOSX and optimized geometries data (ZIP)

■ AUTHOR INFORMATION

Corresponding Author

Alan S. Goldman − *Department of Chemistry and Chemical Biology, Rutgers The State University of New Jersey, New Brunswick, New Jersey 08903, United States;* ⓞ orcid.org/ 0000-0002-2774-710X; Email: alan.goldman@rutgers.edu

Authors

Yansong J. Lu − *Department of Chemistry and Chemical Biology, Rutgers The State University of New Jersey, New Brunswick, New Jersey 08903, United States*

Xiawei Zhang − *Department of Chemistry and Chemical Biology, Rutgers The State University of New Jersey, New Brunswick, New Jersey 08903, United States*

Santanu Malakar − *Department of Chemistry and Chemical Biology, Rutgers The State University of New Jersey, New Brunswick, New Jersey 08903, United States*

Karsten Krogh-Jespersen − *Department of Chemistry and Chemical Biology, Rutgers The State University of New Jersey, New Brunswick, New Jersey 08903, United States*

Faraj Hasanayn − *Department of Chemistry, American University of Beirut, Beirut 1107 2020, Lebanon;* ⓞ orcid.org/ 0000-0003-3308-7854

Complete contact information is available at:
https://pubs.acs.org/10.1021/acs.joc.9b02846

Notes

The authors declare no competing financial interest.
A version of this manuscript was filed on the preprint server ChemRxiv.[35]

■ ACKNOWLEDGMENTS

■ REFERENCES

(1) Crabtree, R. H.; Lei, A. Introduction: CH Activation. *Chem. Rev.* **2017**, *117*, 8481−8482 and references therein.

(2) ((a)) Kumar, A.; Goldman, A. S. Recent Advances in Alkane Dehydrogenation Catalyzed by Pincer Complexes. In *The Privileged Pincer-Metal Platform: Coordination Chemistry & Applications*, van Koten, G.; Gossage, R. A., Eds. Springer International Publishing: Cham, Switzerland, 2016; pp 307−334. (b) Kumar, A.; Bhatti, T. M.; Goldman, A. S. Dehydrogenation of Alkanes and Aliphatic Groups by Pincer-Ligated Metal Complexes. *Chem. Rev.* **2017**, *117*, 12357−12384.

(3) Zhang, X.; Fried, A.; Knapp, S.; Goldman, A. S. Novel Synthesis of Enamines by Iridium-Catalyzed Dehydrogenation of Tertiary Amines. *Chem. Commun.* **2003**, 2060−2061.

(4) Gupta, M.; Hagen, C.; Flesher, R. J.; Kaska, W. C.; Jensen, C. M. A Highly Active Alkane Dehydrogenation Catalyst: Stabilization of Dihydrido Rh and Ir Complexes by a P-C-P Pincer Ligand. *Chem. Commun.* **1996**, 2083−2084.

(5) (a) Adams, J. P. Imines, Enamines and Oximes. *J. Chem. Soc., Perkin Trans. 1* **2000**, 125−139. (b) Guo, F.; Clift, M. D.; Thomson, R. J. Oxidative Coupling of Enolates, Enol Silanes, and Enamines: Methods and Natural Product Synthesis. *Eur. J. Org. Chem.* **2012**, *2012*, 4881−4896. (c) Shi, Z.; Glorius, F. Efficient and Versatile Synthesis of Indoles from Enamines and Imines by Cross-Dehydrogenative Coupling. *Angew. Chem., Int. Ed.* **2012**, *51*, 9220−9222. (d) Ramasastry, S. S. V. Enamine/Enolate-Mediated Organocatalytic Azide-Carbonyl [3+2] Cycloaddition Reactions for the Synthesis of Densely Functionalized 1,2,3-Triazoles. *Angew. Chem., Int. Ed.* **2014**, *53*, 14310−14312.

(6) Gupta, M.; Hagen, C.; Kaska, W. C.; Cramer, R. E.; Jensen, C. M. Catalytic Dehydrogenation of Cycloalkanes to Arenes by a

Dihydrido Iridium P–C–P Pincer Complex. *J. Am. Chem. Soc.* **1997**, *119*, 840–841.

(7) (a) Liu, F.; Goldman, A. S. Efficient Thermochemical Alkane Dehydrogenation and Isomerization Catalyzed by an Iridium Pincer Complex. *Chem. Commun.* **1999**, 655–656. (b) Kundu, S.; Choliy, Y.; Zhuo, G.; Ahuja, R.; Emge, T. J.; Warmuth, R.; Brookhart, M.; Krogh-Jespersen, K.; Goldman, A. S. Rational Design and Synthesis of Highly Active Pincer-Iridium Catalysts for Alkane Dehydrogenation. *Organometallics* **2009**, *28*, 5432–5444. (c) Kumar, A.; Zhou, T.; Emge, T. J.; Mironov, O.; Saxton, R. J.; Krogh-Jespersen, K.; Goldman, A. S. Dehydrogenation of *n*-Alkanes by Solid-Phase Molecular Pincer-Iridium Catalysts High Yields of α-Olefin Product. *J. Am. Chem. Soc.* **2015**, *137*, 9894–9911.

(8) Precursors of (pincer)Ir fragments typically used for catalysis include the corresponding dihydrides, tetrahydrides, the ethylene adduct, and the hydride chloride with addition of strong base (refs 2, 4, 6, and 7). No measurable difference in catalytic activity between these precursors has ever been reported. The tetrahydrides are more easily synthesized and more stable with respect to decomposition than the dihydride, but because of the ease with which the tetrahydrides lose 1 mol of H_2, it is often difficult to isolate tetrahydride free of dihydride; therefore, mixtures of dihydride and tetrahydride are often used. In this work, dihydride, tetrahydride, or mixtures thereof (collectively referred to as "(pincer)IrH$_n$") were used in all cases.

(9) Zhu, K.; Achord, P. D.; Zhang, X.; Krogh-Jespersen, K.; Goldman, A. S. Highly Effective Pincer-Ligated Iridium Catalysts for Alkane Dehydrogenation. DFT Calculations of Relevant Thermodynamic, Kinetic, and Spectroscopic Properties. *J. Am. Chem. Soc.* **2004**, *126*, 13044–13053.

(10) ((a)) *Enamines: Synthesis, Structure and Reactions*; 2nd Ed.; Cook, A. G., Ed. Marcel Dekker: New York, 1988. (b) Adams, J. P.; Robertson, G. Imines, enamines and related functional groups. *Contemp. Org. Synth.* **1997**, *4*, 183–195.

(11) *Cycloaddition Reactions in Organic Synthesis*, Kobayashi, S.; Jørgensen, K. A., Eds.; Wiley-VCH Verlag GmbH: Weinheim, Germany, 2001.

(12) (a) Simmons, H. E.; Smith, R. D. A New Synthesis Of Cyclopropanes From Olefins. *J. Am. Chem. Soc.* **1958**, *80*, 5323–5324. (b) Lebel, H.; Marcoux, J.-F.; Molinaro, C.; Charette, A. B. Stereoselective Cyclopropanation Reactions. *Chem. Rev* **2003**, *103*, 977–1050. (c) Charette, A. B.; Beauchemin, A. Simmons-Smith Cyclopropanation Reaction. *Org. React.* **2004**, 1–415.

(13) Hoyt, J. M.; Schmidt, V. A.; Tondreau, A. M.; Chirik, P. J. Iron-catalyzed intermolecular [2+2] cycloadditions of unactivated alkenes. *Science* **2015**, *349*, 960–963.

(14) Stanley, L. M.; Sibi, M. P. Enantioselective Copper-Catalyzed 1,3-Dipolar Cycloadditions. *Chem. Rev.* **2008**, *108*, 2887–2902.

(15) (a) Esquivias, J.; Arrayás, R. G.; Carretero, J. C. Catalytic Asymmetric Inverse-Electron-Demand Diels–Alder Reaction of N-Sulfonyl-1-Aza-1,3-Dienes. *J. Am. Chem. Soc.* **2007**, *129*, 1480–1481. (b) Akiyama, T.; Morita, H.; Fuchibe, K. Chiral Brønsted Acid-Catalyzed Inverse Electron-Demand Aza Diels–Alder Reaction. *J. Am. Chem. Soc.* **2006**, *128*, 13070–13071.

(16) Typical reaction conditions included 10 mM catalyst, 100 mM substrate, and 200 mM hydrogen acceptor in *p*-xylene-*d*$_{10}$ solvent.

(17) Loss of NBE was determined by ^{1}H NMR spectroscopy, while the formation of a thread-like precipitate was observed.

(18) Zhang, X.; Kanzelberger, M.; Emge, T. J.; Goldman, A. S. Selective Addition to Iridium of Aryl C-H Bonds Ortho to Coordinating Groups Not Chelation-Assisted. *J. Am. Chem. Soc.* **2004**, *126*, 13192–13193.

(19) (a) West, N. M.; White, P. S.; Templeton, J. L. Facile dehydrogenation of ethers and alkanes with aβ-diiminate Pt fragment. *J. Am. Chem. Soc.* **2007**, *129*, 12372–12373. (b) Whited, M. T.; Zhu, Y.; Timpa, S. D.; Chen, C.-H.; Foxman, B. M.; Ozerov, O. V.; Grubbs, R. H. Probing the C-H Activation of Linear and Cyclic Ethers at (PNP)Ir. *Organometallics* **2009**, *28*, 4560–4570.

(20) Lyons, T. W.; Bézier, D.; Brookhart, M. Iridium Pincer-Catalyzed Dehydrogenation of Ethers Featuring Ethylene as the Hydrogen Acceptor. *Organometallics* **2015**, *34*, 4058–4062.

(21) Yao, W.; Zhang, Y.; Jia, X.; Huang, Z. Selective Catalytic Transfer Dehydrogenation of Alkanes and Heterocycles by an Iridium Pincer Complex. *Angew. Chem., Int. Ed.* **2014**, *53*, 1390–1394.

(22) As noted, the (^{tBu4}PCP)Ir fragment requires milder conditions for catalysis and it allows the use of precursors such as (^{tBu4}PCP)Ir(Ph)(H) at even milder conditions. Given that the same selectivity patterns of selectivity were observed for both (^{tBu4}PCP)Ir (**1**) and (^{iPr4}PCP)Ir (**2**), we decided to use **1** for all mechanistic studies.

(23) Kanzelberger, M.; Singh, B.; Czerw, M.; Krogh-Jespersen, K.; Goldman, A. S. Addition of C-H Bonds to the Catalytically Active Complex (PCP)Ir (PCP = η^3-2,6-(R$_2$PCH$_2$)$_2$C$_6$H$_3$). *J. Am. Chem. Soc.* **2000**, *122*, 11017–11018.

(24) (a) Jones, W. D.; Feher, F. J. Isotope effects in arene carbon-hydrogen bond activation by [(C$_5$Me$_5$)Rh(PMe$_3$)]. *J. Am. Chem. Soc.* **1986**, *108*, 4814–4819. (b) Jones, W. D. Isotope effects in C-H bond activation reactions by transition metals. *Acc. Chem. Res.* **2003**, *36*, 140–146. (c) Churchill, D. G.; Janak, K. E.; Wittenberg, J. S.; Parkin, G. Normal and Inverse Primary Kinetic Deuterium Isotope Effects for C-H Bond Reductive Elimination and Oxidative Addition Reactions of Molybdenocene and Tungstenocene Complexes: Evidence for Benzene σ-Complex Intermediates. *J. Am. Chem. Soc.* **2003**, *125*, 1403–1420. (d) Janak, K. E.; Parkin, G. Temperature-Dependent Transitions between Normal and Inverse Equilibrium Isotope Effects for Coordination and Oxidative Addition of C-H and H-H Bonds to a Transition Metal Center. *J. Am. Chem. Soc.* **2003**, *125*, 6889–6891.

(25) The calculations of the β-hydride TSs for pathways **a** and **b** were also conducted at the M06L level with the def2tzvp basis set on the main group elements and the def2qzvp basis set and associated ECP on Ir (ref 28). With this method, the free energy for pathway **b** at 323 K was calculated to be 0.5 kcal/mol lower than that for pathway **a**. As found with the computational method used throughout this work, the KIEs calculated by this method for pathway **b** (and not for pathway **a**) are consistent with the experimental results. The KIEs given are based on vibrational frequencies scaled by 0.95. Specifically, $k(C_2H_5)/k(CH_2CD_3) = 3.5$, $k(C_2H_5)/k(CD_2CH_3) = 2.8$ (50 °C), and $k(C_2H_5)/k(C_2D_5) = 7.7$ (90°C) as compared with respective experimental values of 3.7, 2.0, and 7.0. (For pathway **a**, the respective calculated KIEs are 2.5, 4.7, and 8.9.) While the calculated difference, $\Delta\Delta G^\ddagger = 0.5$ kcal/mol favoring pathway **b**, is in the direction consistent with the experiment, the magnitude is too small to explain all experimental results since it would imply (if taken at the face value) that the reaction would operate through both pathways at comparable rates (with pathway **b** predominating by a factor of only 2.2). However, even a difference of only 1.0 kcal/mol would result in one pathway predominating by a factor of 5.

(26) (a) Schuchardt, K. L.; Didier, B. T.; Elsethagen, T.; Sun, L.; Gurumoorthi, V.; Chase, J.; Li, J.; Windus, T. L. Basis Set Exchange: A Community Database for Computational Sciences. *J. Chem. Inf. Model.* **2007**, *47*, 1045–1052. (b) Feller, D. The role of databases in support of computational chemistry calculations. *J. Comput. Chem.* **1996**, *17*, 1571–1586. ((c)) https://bse.pnl.gov/bse/portal. Accessed Sep 2019.

(27) Kuffner, F.; Koechlin, W. Highly branched aliphatic compounds. IV. Preparatively useful syntheses of triisopropylamine. *Monatsh. Chem.* **1962**, *93*, 476–482.

(28) Koch, W.; Holthausen, M. C. *A Chemist's Guide to Density Functional Theory*; Wiley: New York, 2001, DOI: 10.1002/3527600043.

(29) Frisch, M. J.; Trucks, G. W.; Schlegel, H. B.; Scuseria, G. E.; Robb, M. A.; Cheeseman, J. R.; Scalmani, G.; Barone, V.; Petersson, G. A.; Nakatsuji, H.; Li, X.; Caricato, M.; Marenich, A. V.; Bloino, J.; Janesko, B. G.; Gomperts, R.; Mennucci, B.; Hratchian, H. P.; Ortiz, J. V.; Izmaylov, A. F.; Sonnenberg, J. L.; Williams-Young, D.; Ding, F.; Lipparini, F.; Egidi, F.; Goings, J.; Peng, B.; Petrone, A.; Henderson, T.; Ranasinghe, D.; Zakrzewski, V. G.; Gao, J.; Rega, N.; Zheng, G.; Liang, W.; Hada, M.; Ehara, M.; Toyota, K.; Fukuda, R.; Hasegawa, J.;

Ishida, M.; Nakajima, T.; Honda, Y.; Kitao, O.; Nakai, H.; Vreven, T.; Throssell, K.; Montgomery, J. A.; Peralta, J. E.; Ogliaro, F.; Bearpark, M. J.; Heyd, J. J.; Brothers, E. N.; Kudin, K. N.; Staroverov, V. N.; Keith, T. A.; Kobayashi, R.; Normand, J.; Raghavachari, K.; Rendell, A. P.; Burant, J. C.; Iyengar, S. S.; Tomasi, J.; Cossi, M.; Millam, J. M.; Klene, M.; Adamo, C.; Cammi, R.; Ochterski, J. W.; Martin, R. L.; Morokuma, K.; Farkas, O.; Foresman, J. B.; Fox, D. J. *Gaussian 16*; Revision A.03, Gaussian, Inc.: Wallingford, CT, 2016.

(30) Yu, H. S.; He, X.; Li, S. L.; Truhlar, D. G. MN15: A Kohn−Sham global-hybrid exchange−correlation density functional with broad accuracy for multi-reference and single-reference systems and noncovalent interactions. *Chem. Sci.* **2016**, *7*, 5032−5051.

(31) (a) Andrae, D.; Häußermann, U.; Dolg, M.; Stoll, H.; Preuß, H. Energy-adjustedab initio pseudopotentials for the second and third row transition elements. *Theor. Chim. Acta* **1990**, *77*, 123−141. (b) Bergner, A.; Dolg, M.; Küchle, W.; Stoll, H.; Preuß, H. Ab initio energy-adjusted pseudopotentials for elements of groups 13-17. *Mol. Phys.* **1993**, *80*, 1431−1441.

(32) (a) Ditchfield, R.; Hehre, W. J.; Pople, J. A. Self-consistent molecular-orbital methods. IX. Extended Gaussian-type basis for molecular-orbital studies of organic molecules. *J. Chem. Phys.* **1971**, *54*, 724−728. (b) Hariharan, P. C.; Pople, J. A. Accuracy of AH_n equilibrium geometries by single determinant molecular orbital theory. *Mol. Phys.* **1974**, *27*, 209−214. (c) Raghavachari, K.; Binkley, J. S.; Seeger, R.; Pople, J. A. Self-consistent molecular orbital methods. XX. A basis set for correlated wave functions. *J. Chem. Phys.* **1980**, *72*, 650−654. (d) McLean, A. D.; Chandler, G. S. Contracted Gaussian basis sets for molecular calculations. I. Second row atoms, Z=11−18. *J. Chem. Phys.* **1980**, *72*, 5639−5648.

(33) Marenich, A. V.; Cramer, C. J.; Truhlar, D. G. Universal Solvation Model Based on Solute Electron Density and on a Continuum Model of the Solvent Defined by the Bulk Dielectric Constant and Atomic Surface Tensions. *J. Phys. Chem. B* **2009**, *113*, 6378−6396.

(34) McQuarrie, D. A. *Statistical Thermodynamics*; Harper and Row: New York, 1973.

(35) Zhang, X.; Malakar, S.; Krogh-Jespersen, K.; Hasanayn, F.; Goldman, A. S. Formation of Enamines via Catalytic Dehydrogenation by Pincer-Iridium Complexes. *ChemRxiv* **2020**, DOI: 10.1021/acs.joc.9b02846.